
ENHANCED HEATING OF SALTY ICE AND WATER UNDER MICROWAVES: MOLECULAR DYNAMICS STUDY

Motohiko Tanaka* and Motoyasu Sato

Coordination Research Center, National Institute for Fusion Science
Oroshi-cho, Toki 509-5292, Japan
Phone: +81-572-58-2258
*mtanaka@nifs.ac.jp

Through the use of molecular dynamics simulations, we have studied the enhanced heating of salty ice and water by the electric field of applied microwaves at 2.5 GHz, and in the range of 2.5-10 GHz for the frequency dependence. We show that water molecules in salty ice are allowed to rotate in response to the microwave electric field to the extent comparable to those in pure water because the molecules in salty ice are loosely tied by hydrogen bonds with adjacent molecules unlike rigidly bonded pure ice. The weakening of hydrogen-bonded network of molecules in salty ice is mainly due to the electrostatic effect of salt ions rather than the short-range geometrical (size) effect of salt since the presence of salt ions with small radii causes similar enhanced heating.

Submission Date: 24 September 2007

Acceptance Date: 18 April 2008

Publication Date: 7 November 2008

INTRODUCTION

Microwaves are frequently utilized as a highly efficient and less carbon-oxide releasing energy source for cooking or drying food, sintering metals and ceramics. It is known that dielectric materials including pure and salty water are heated efficiently by absorbing the electric field energy of microwaves [von Hippel, 1954; Hobbs *et al.*, 1966; Hasted, 1972; Buchner, 1999; Meissner and Wentz, 2004; Takei, 2007]. It is also known that metallic powders and magnetic materials such as magnetite and titanium oxides with oxygen defects TiO_{2-x} ($x>0$) are heated by the magnetic field of microwaves [Roy *et al.*, 1999; Peelamedu *et al.*, 2002; Sato

et al., 2006; Suzuki *et al.*, 2008; Tanaka *et al.*, 2008].

In order to examine the mechanism of microwave heating of water and ice at the molecular level, we performed molecular dynamics simulations [Tanaka and Sato, 2007]. Through the simulations we showed mechanistically that (i) rotational excitation of electric dipoles of water coupled with irreversible energy relaxation to the translational energy was responsible for the microwave heating of water, (ii) pure ice was not heated by microwaves because of strong hydrogen bonds between water molecules, and (iii) the experimentally known enhanced heating of salt water by microwaves was due to acceleration of salt ions by the microwave electric field, which is usually termed as Joule heating. We numerically evaluated the time

Keywords: Microwave heating, salty water and ice, electrostatic effects, molecular dynamics

integrated Joule heating term of salt ions, $\mathbf{E} \cdot \mathbf{J}$, and the work associated with rotation of electric dipoles, $\mathbf{E} \cdot d\mathbf{P}$, by summing up the contribution of all atoms or molecules, where \mathbf{E} is the electric field of microwaves, $\mathbf{J} = \sum_i q_i \mathbf{v}_i$ is the current carried by Na^+ and Cl^- ions, and $\mathbf{P} = \sum_s \mathbf{d}_s$ is the sum of electric dipoles of all water molecules, with q_i and \mathbf{v}_i the charge and velocity of the i -th atom, respectively, and \mathbf{d}_s the electric dipole moment of the s -th molecule. We obtained the relation $|\mathbf{E} \cdot \mathbf{J}| \approx 2 |\mathbf{E} \cdot d\mathbf{P}/dt|$ for dilute saline solution of 1 mol% salinity and 10 GHz microwave [Tanaka and Sato, 2007].

We stated previously that pure ice is not heated by microwaves. However, we have a daily experience of processing (melting) frozen food in microwave ovens. Our motivation for the present work is to examine the heating of salty ice as well as salty water by molecular dynamic simulation. In this paper we mainly use microwaves with 2.5 GHz, except for 5-10 GHz microwaves for examining the frequency dependence of the heating.

SIMULATION PROCEDURES

Ice and liquid water are characterized by a completely and partially ordered network of H_2O molecules, respectively, mediated by hydrogen bonds connecting adjacent two molecules [Matsumoto *et al.*, 2002]. For this reason, we adopt an explicit water model with three point charges – the SPC/E water model [Toukan and Rahman, 1985; Berendsen *et al.*, 1987]. A typical simulation run requires the computation time of a few days for roughly 3000 water molecules on our Opteron-based cluster machine. Although the model has reasonable electrostatic properties, for a more accurate calculation of the energy absorption, the use of TIP4P-FQ model with polarization effect [English and MacElroy, 2003; English, 2006] may be preferred but with a small number of water molecules due to large computation

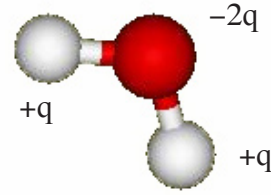


Figure 1. Three-atom rigid-body model for a water molecule (SPC/E model) with partial charges on atom sites.

times.

We follow the same numerical procedures as those used previously [Tanaka and Sato 2007]. We start all the simulations with the crystal ice and relax it to the desired temperature before microwaves are applied. This is done because molecules of initially random orientations take a very long time to arrive at the equilibrium with properly ordered hydrogen-bonded network. A water molecule of the SPC/E model in Figure 1 illustrates that three atoms form a rigid triangle H-O-H with partial charges q ($=0.424e$) and $-2q$ residing at the hydrogen and oxygen sites, respectively. The electrostatic forces are calculated for pairs of these atoms while the Lennard-Jones forces are calculated only for the pairs of oxygen atoms. The equations of motion are:

$$m_i \frac{d\mathbf{v}_i}{dt} = -\nabla \left[\sum_j \frac{q_i q_j}{r_{ij}} + 48\epsilon_{ij} \left\{ \left(\frac{\sigma_{ij}}{r_{ij}} \right)^{12} - \left(\frac{\sigma_{ij}}{r_{ij}} \right)^6 \right\} \right] + q_i \mathbf{E}_{mw}, \quad (1)$$

$$\frac{d\mathbf{r}_i}{dt} = \mathbf{v}_i. \quad (2)$$

Here, \mathbf{r}_i and \mathbf{v}_i are the position and velocity of the i -th atom, respectively, m_i and q_i are its mass and charge, respectively, and $r_{ij} = |\mathbf{r}_i - \mathbf{r}_j|$ is the distance between i -th and j -th atoms. The second term in the bracket on the right-hand side of Eq.(2) serves for two atoms not to overlap each other, where σ_{ij} is the sum of radii of two

atoms and ϵ_{ij} is the Lennard-Jones energy. For water, $\epsilon_{ww} = 0.65$ kJ/mol and $\sigma_{ww} = 0.317$ nm. Salt ions are put randomly in space avoiding water molecules and are treated as isolated species with the charge $q_{Na} = e$, the diameter $2\sigma_{Na} = 0.267$ nm and the Lennard-Jones energy $\epsilon_{Na} = 0.062$ kJ/mol for Na^+ , and $q_{Cl} = -e$, $2\sigma_{Cl} = 0.44$ nm and $\epsilon_{Cl} = 0.446$ kJ/mol for Cl^- [AMBER, 2008]; the hybrid rule

$$\epsilon_{ij} = (\epsilon_i \epsilon_j)^{1/2}, \quad \sigma_{ij} = \sigma_i + \sigma_j \quad (3)$$

is used when two species i and j are encountering. The diameter of Cl^- ion is comparable with the size of the network cell whose building blocks are six-membered water rings. The SHAKE and RATTLE algorithm [Andersen, 1983] is adopted in time integration of Eq.(1) and (2) to keep the rigid triangular shape of the molecule. The time step for integration is 1 fs.

Our simulation system consists of a cubic box of each side 4.2 nm that contains $(14)^3$ water molecules when salt is not added. The periodic boundary condition is imposed under the constant system volume. Thus, the Ewald sum for infinite number of periodic image charges is taken to correctly account for the electric field in which the particle-particle particle-mesh algorithm is adopted [Deserno and Holm, 1998]. The real space cutoff distance for both the electrostatic and Lennard-Jones forces is 1.0 nm, and 32 spatial grids are used for the Fourier-space calculation of the nonlocal electrostatic forces.

After an equilibration phase of 100 ps, a spatially homogeneous microwave electric field of the form $\mathbf{E}_{mw}(t) = E_0 \omega t \hat{\mathbf{x}}$ is applied. The wave frequency $f = \omega/2\pi$ is 2.5 GHz unless otherwise specified. To overcome the numerical noises in the simulation, the used wave amplitude is $E_0 = 2.3 \times 10^6$ V/cm which is large but its associated energy with the electric dipole of a water molecule is less than the thermal energy at room temperature $E_0 d / k_B T_{300K} \approx 0.4$. This condition assures us the safe use of this electric field in

our simulations, where $d \approx 7.8 \times 10^{-30}$ is the dipole moment of the model water molecule.

RESULTS AND DISCUSSION

The initial condition of the simulation is prepared by generating crystal ice of the I_c structure, and adding Na and Cl ions of 1 mol% concentration (roughly 3 wt%) when salty ice or water is prepared. The I_c ice is isotropic in three directions whose physical properties are quite similar to those of the ordinary ice of the I_h structure [Eisenberg and Kauzman, 1969; Matsumoto *et al.*, 2002]; we swap the O-H bonds of water molecules successively until an isotropic state has been reached. The initial structure is equilibrated for 100 ps at a given temperature, and then the microwave electric field of 2.5 GHz frequency is applied.

Figure 2 shows the time history of (a) the temperature (starting at 230 K) of the salty ice system, (b) time integrated value of the Joule heating and dipole heating terms, (c) the average velocity of Na^+ along the x direction, and (d) that of Cl^- . It is noted that the temperature of salty ice increases monotonically after the microwave is turned on. The velocities of salt ions in panels (c) and (d) remain small compared to those in salty water in Figure 3 until the ice approaches the melting temperature. To clarify the heating mechanism, the Joule heating term $\mathbf{E} \cdot \mathbf{J}$ (dotted and dashed lines for the total salt and Na^+ , respectively) and the dipole heating term $\mathbf{E} \cdot d\mathbf{P}/dt$ (solid line) are plotted separately in (b). Evidently, the excitation of dipole rotation is the principal heating mechanism of salty ice.

The heating of salty ice is compared with that of salty water in Figure 3. Salty water with 1 mol% salinity is prepared in the same way as for salty ice, and is melted and equilibrated for 100 ps at 300 K. For the salty water, the heating rate increases with a temperature above 350 K, as seen in Figure 3(a) at which the slope of the curve becomes steeper. The velocity oscillations of Na and Cl ions in (c) and (d) also

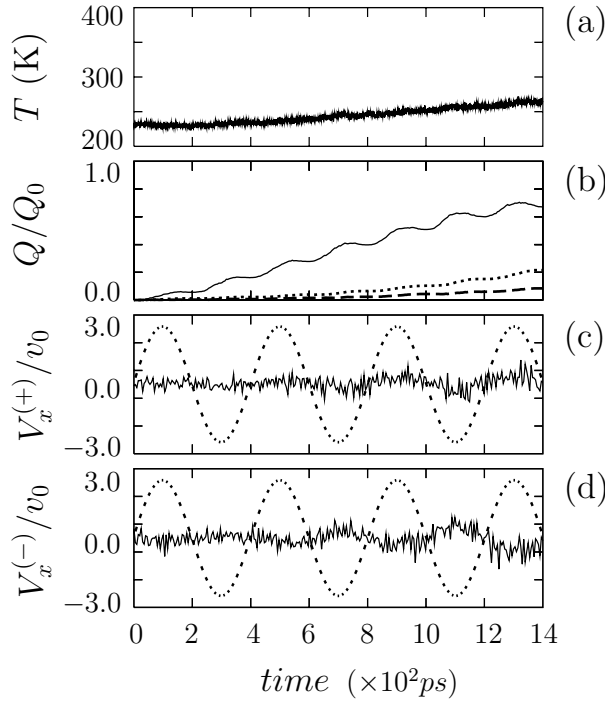


Figure 2. The time history of the heating of salty ice, (a) temperature of the whole system in Kelvin, (b) the dipole heating term (solid line), the Joule heating term of all salt (dotted) and that of Na ion (dashed), (c) the x-component velocity of Na ions, and (d) that of Cl ions with $v_0=10\text{m/s}$, $Q_0=10^{-9}\text{J/s}$. The amplitude of the microwave electric field is shown by dotted lines in (c) and (d), where the electric field of 2.5 GHz is turned on just after the equilibration phase at time 0 of the figure.

increase in time and are much larger than those for salty ice. The large oscillations at later times reveal de-trapping of salt ions from the cell of the water network, which accelerates the heating due to large oscillations. A striking difference is found in the heating terms in panel (b): the Joule heating term much exceeds the dipole heating term, where the former is twice as big as the latter as shown previously [Tanaka and Sato, 2007]. It is interesting that Cl ions with a heavier mass and a larger radius respond more than Na ions to the microwave electric field. This implies that Cl ions are not stably contained in the cells of the hydrogen-bonded network of water molecules, which makes them more easily to be de-trapped

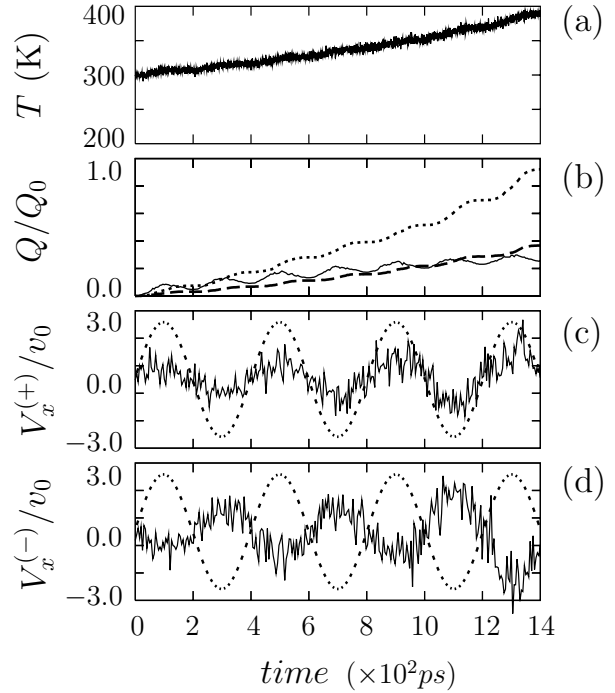


Figure 3. The time history of the heating of salty water, (a) temperature of the whole system in Kelvin, (b) the dipole heating term (solid line), the Joule heating term of all salt (dotted) and that of Na ion (dashed), (c) the x-component velocity of Na ions, and (d) that of Cl ions with $v_0=10\text{m/s}$ and $Q_0=10^{-9}\text{J/s}$. The amplitude of the microwave electric field is shown by dotted lines in (c) and (d), where the electric field is turned on just after the equilibration phase at time 0 of the figure.

and move through the network.

As for reference, the heating of pure water against 2.5 GHz microwave is shown in Figure 4. In this case, the excitation of dipole rotation is the only mechanism of energy absorption from the microwave. The heating rate of salty ice with 1 mol% salinity is comparable to that for pure water. The velocity oscillations are shown for (c) hydrogen atoms and (d) oxygen atoms, which are small compared with those in Figure 3 and are out of phase with each other since the center of the mass of water molecules is fixed because of the charge neutrality.

As pure ice is not heated by microwaves

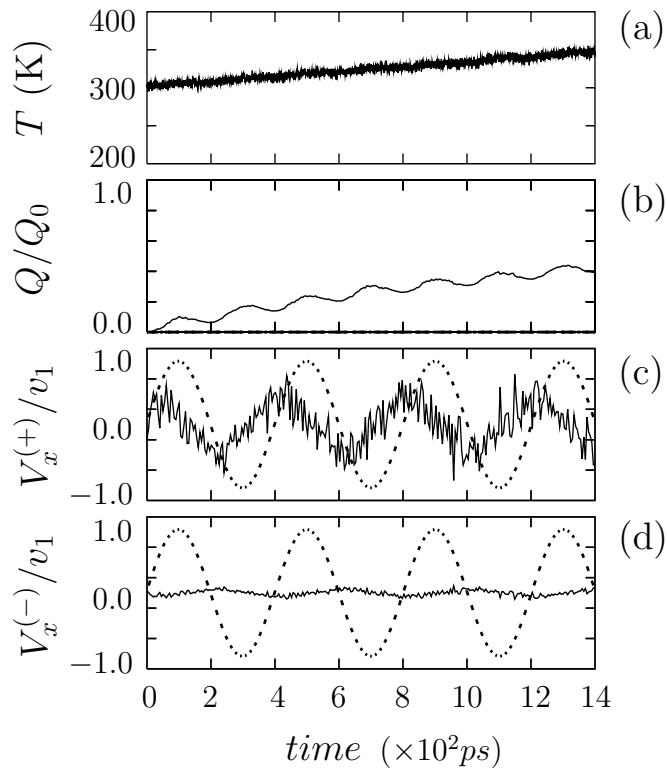


Figure 4. The time history of the heating of pure water, (a) temperature in Kelvin, (b) the dipole heating term, (c) the x -component velocity of hydrogen atoms, and (d) that of oxygen atoms with $v_1=1\text{m/s}$ and $Q_0=10^9\text{ J/s}$. The amplitude of the microwave electric field is shown by dotted lines in (c) and (d), where the electric field of 2.5 GHz is turned on just after the equilibration phase at time 0 of the figure.

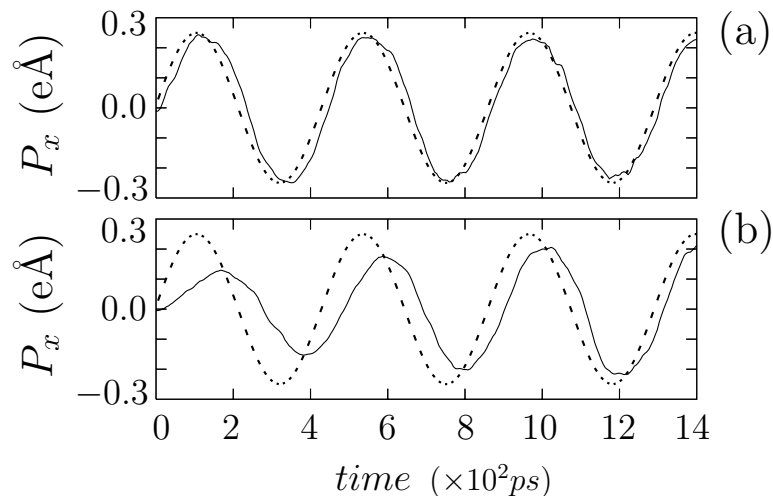


Figure 5. Time history of the sum of all electric dipoles in the x direction for (a) pure water (corresponding to Figure 4) and (b) salty ice (Figure 2). Solid lines show the value of electric dipoles, and dashed lines show the amplitude of the electric field of microwaves.

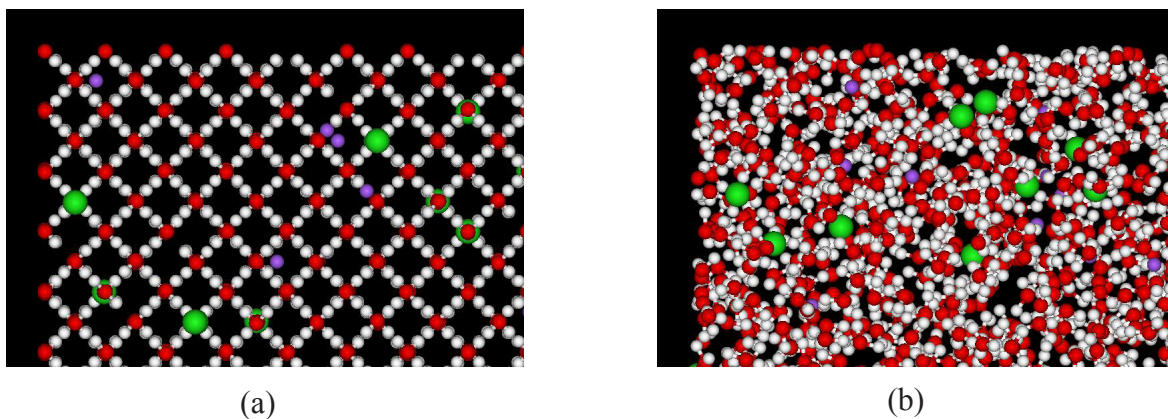


Figure 6. (color online) 3D view of water molecules and salt ions for salty ice (230 K) at (a) the initial stage, and (b) after 100 ps without microwave application. Chained gray and white spheres represent oxygen and hydrogen atoms, respectively. Na and Cl ions are shown by isolated small and large spheres, respectively.

of the GHz band, the presence of salt in ice should play a decisive role in the heating (melting) process in the microwave electric field. We showed on the energy basis in Figure 2 that it was not the Joule heating, but the excitation of dipole rotation that is responsible for the heating. It follows that electric dipoles of water molecules are allowed to rotate in salty ice, which occurs because of the local breaking of water network by salt ions. This is well recognized in Figure 5 which shows the time history of the sum of the electric dipoles for (a) pure water and (b) salty ice. For pure water, molecules begin rotational motions immediately with the microwave electric field. In the early phase when microwaves are applied to salty ice, the rotational motion of the dipoles begins which is somewhat retarded and small compared to the case of pure water. This is completely different from the case of pure ice.

Figure 6 shows that the rigid network of ice is distorted quickly in the presence of salt ions even before microwave is applied, as seen in (b). Experimentally, anomalously high permittivity was reported for salty ice [Zhong *et al.*, 1988]. Here, it is confirmed by numerical simulation at the molecular level that the high response of salty ice to microwaves is caused by the presence of salt ions in ice which weaken

the hydrogen-bonded rigid network of water molecules.

The weakening of the hydrogen-bonded network of water molecules which occurs in salty ice is also confirmed by specially designed simulation: the diameter of charged salt ions is artificially reduced to 0.2 nm so that they fit nicely in the cell of the network. Even in such a condition, heating of salty ice does occur, and the heating rate is almost three quarters that of the normal case. This proves that the weakening of the network in salty ice is caused mainly by the electrostatic effect of salt ions which is long-ranged, rather than the short-range geometrical effect.

The dependence of the heating rate on the microwave's frequency is examined for pure and salty water and salty ice, as depicted in Figure 7. Microwaves of three frequencies 2.5, 5 and 10 GHz are used, and the temperature increase in the 1.4 ns interval is plotted for pure water (filled circles), salty water (open circles) and salty ice (triangles). The salinity of salty ice and water is 1 mol%, and initial temperature is 300 K for water and 230 K for ice. The line fitting yields the frequency dependence of $dT/dt \propto \omega^{1.4}$ and $\omega^{1.2}$ for pure water and salty ice, respectively. For salty water, we obtain $dT/dt \propto \omega^{0.7}$. The proximity of the scaling laws for

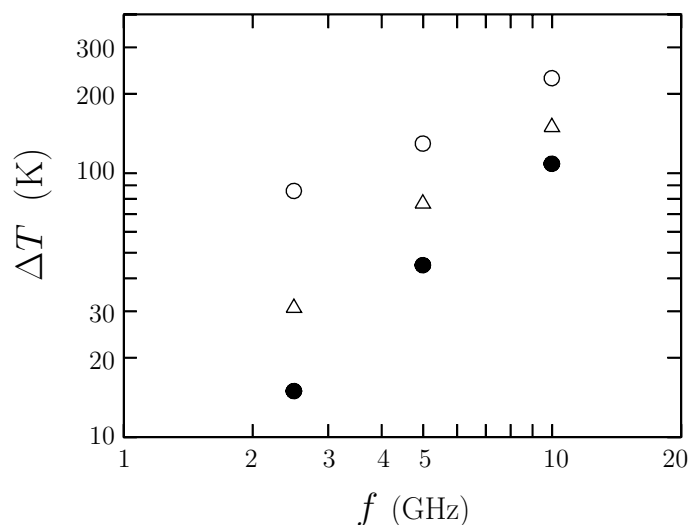


Figure 7. The dependence of heating rate on microwave frequency. Open circles and triangles correspond to salty water and salty ice with 1 mol% salinity, respectively, and filled circles correspond to pure water at 300 K.

pure water and salty ice indicates that water molecules in salty ice under microwaves rotate as freely as those in pure water.

SUMMARY

Through molecular dynamics simulation, we studied the heating process of salty ice, which we encounter daily when we melt frozen food in a microwave oven. We confirmed that the heating of salty ice is attributed to the weakening of the hydrogen-bonded network of water molecules in the presence of charged salt ions. In this process, the electrostatic effect was dominant over the short-range geometrical effect. The dependence of the heating rate on microwave frequency was examined for salty ice and water, which again indicated that the internal structure of water molecules in salty ice is deformed. Thus, the water molecules in salty ice can rotate as freely as those in pure water under the microwave electric field.

ACKNOWLEDGMENTS

The authors thank Dr. M. Matsumoto for fruitful discussions on the structure of ice. This work was supported by the Grant-in-Aid

No.18070005 (FY2006-2010) from the Japan Ministry of Education, Science and Culture for Prime Area Research Project “Science and Technology of Microwave-Induced Thermally Non-Equilibrium Reaction Fields”. Present computation was performed using our cluster machine consisting of 64-cpu Opteron 254 (2.8 GHz, single core) processors and high-speed InfiniBand interconnect.

REFERENCES

- AMBER database and molecular dynamics code ("Assisted Model Building with Energy Refinement"), ver.10 (2008), at <http://amber.scripps.edu>.
- Andersen, H.C. (1983). “Rattle: a velocity version of the Shake algorithm for molecular dynamics calculations.” *J. Comput. Phys.*, 52, pp.24-34.
- Berendsen, H., J. Grigela and T. Straatsma (1987). “The missing term in effective pair potential.” *J. Phys. Chem.*, 91, pp.6269-6271.
- Buchner, R., J. Barthel and J. Stauber (1999). “The dielectric relaxation of water between 0°C and 35°C.” *Chem. Phys. Lett.*, 306, pp.57-63.
- Deserno, M. and Holm, C. (1998). "How to mesh up Ewald sums. II. An accurate error estimate for the particle-particle-particle-mesh algorithm." *J. Chem. Phys.*, 109,

-
- pp.7678.
- (1954). Dielectric Materials and Applications, edited by A.R. von Hippel. MIT Press, Cambridge, USA.
- Eisenberg, D. and W. Kauzman (1969). The Structure and Properties of Water. Oxford University Press, London.
- English, N.J. and J.M. MacEloy (2003). "Hydrogen bonding and molecular mobility in liquid water in external electromagnetic fields." *J. Chem. Phys.*, 119, pp.11806-11813.
- English, N.J. (2006). "Molecular dynamics simulations of microwave effects on water using different long-range electrostatics methodologies." *Mol. Phys.*, 104, pp.243-253 and references therein.
- Hasted, J.B. (1972). "Liquid water: Dielectric properties." in Water: A Comprehensive Treatise., vol. 1, edited by F. Franks. Plenum Press, New York, pp.255-309.
- Hobbs, M.E., M.S. Jhon and H. Eyring (1966). "The dielectric constant of liquid water and various forms of ice according to significant structure theory." *Proc. Nat. Acad. Sci.*, 56, pp.31-38.
- Matsumoto, M., S. Saito and I. Ohmine (2002). "Molecular dynamics simulation of the ice nucleation and growth process leading to water freezing." *Nature*, 416, pp.409-413.
- Meissner, T. and F.J. Wentz (2004). "The complex dielectric constant for pure and sea water from microwave satellite observations." *IEEE Trans. Geosci. Remote Sensing*, 42, pp.1836-1849.
- Peelamedu, R.D., M. Fleming, D.K. Agrawal and R. Roy (2007). "Preparation of titanium nitride: Microwave-induced carbothermal reaction of titanium dioxide." *J. Amer. Ceramic Soc.*, 85, pp.117-120.
- Roy, R., D. Agrawal, J. Cheng and S. Gedevarishvili (1999). "Full sintering of powdered-metal bodies in a microwave field." *Nature*, 399, pp.668-670.
- Sato, M. et al. "Science and Technology of Microwave-Induced, Thermally Non-Equilibrium Reaction Fields." Grant-in-Aid for Prime Area Research from the Japan Ministry of Education, Science and Culture (FY 2006-2010), see <http://phonon.nifs.ac.jp>.
- Suzuki, M., M. Ignatenk, M. Yamashiro, M. Tanaka and M. Sato (2008). "Numerical study of microwave heating of micrometer size metal particles." *ISIJ Intern'l.*, 48, pp.681-684.
- Takei, I. (2007). "Dielectric relaxation of ice samples grown from vapor-phase or liquid-phase water." Physics and Chemistry of Ice, edited by W. Kuhs. Royal Society of Chemistry, Cambridge, pp.577-584.
- Tanaka, M. and M. Sato (2007). "Microwave heating of water, ice and saline solution: Molecular dynamics study." *J. Chem. Phys.*, 126, 034509, pp.1-9.
- Tanaka, M., H. Kono and K. Maruyama (2008). "Selective heating mechanism of magnetic metal oxides by microwave magnetic field." Archive (arxiv) cond-mat/08063055.
- Toukan, K. and A. Rahman (1985). "Molecular-dynamics study of atomic motions in water." *Phys. Rev.*, B31, pp.2643-2648.
- Zhong, L., C. Xu and C. Qiu (1988). "Anomalous high permittivity in salty ice – a new dielectric phenomenon." *Proc. Properties and Applications of Dielectric Materials*, 1, pp.206-208.